# Array Self Calibration with Large Sensor Position Errors

Brian P. Flanagan

*The MITRE Corporation, 11493 Sunset Hills Rd., Reston, VA 20190, USA, bflan@mitre.org*

Kristine L. Bell

*Dept. of Appl. and Eng. Statistics, George Mason University, Fairfax, VA 22030-4444, USA, kbell@gmu.edu*

**Abstract**

Self-calibration algorithms estimate both source directions-of-arrival (DOAs) and perturbed array response vector parameters, such as sensor locations. Calibration errors are usually assumed to be small and a first order approximation to the perturbed array response vector is often used to simplify the estimation procedure. In this paper, we develop a more robust procedure that does not rely on the small error assumption. It has better performance for large estimation errors, and when used to initialize the Weiss and Friedlander MUSIC-based iterative technique, we see significant improvement over existing techniques for both small and large errors.

## 1 Introduction

A common application in antenna array processing is direction of arrival (DOA) estimation for closely spaced sources. A number of algorithms exist for solving this problem. Research has shown that these algorithms can be very sensitive to errors in the antenna array, including gain/phase deviations, sensor location errors, and mutual coupling errors [1]-[9].

There are a number of techniques available for calibrating the array. The simplest techniques require sources with known DOAs [10]-[22]. This may not be realistic in many situations, and we'd prefer to use an algorithm that doesn't require any known sources, but instead relies entirely on targets of opportunity. Several examples of this class of algorithms, known as self calibration algorithms, have been proposed in recent years to correct for gain/phase [2], [3],

[6], [23]-[31], mutual coupling [3], and sensor location errors [3], [30]-[34]. Two techniques that we study in detail in this paper were developed by Weiss and Friedlander [32] and Viberg and Swindlehurst [31]. The Weiss and Friedlander (WF) technique is based on the MUSIC algorithm and alternately estimates the DOAs and the sensor locations until convergence is achieved. The Viberg and Swindlehurst technique uses a maximum a posteriori noise subspace fitting (MAP-NSF) method which estimates all parameters simultaneously by using a Bayesian approach.

Another approach to this problem is to avoid calibration altogether by designing DOA estimation techniques which are less sensitive to calibration errors [6], [23], [35]-[42]. Examples of these techniques are the weighted subspace fitting (WSF) and optimal subspace fitting (OSF) techniques introduced by Viberg and Swindlehurst [6]. These are multi-dimensional techniques that apply weighting matrices to a cost function to reduce the sensitivity to calibration errors. An improvement to the WSF algorithm was introduced by Jansson, Swindlehurst, and Ottersten [23] to provide greater performance against correlated signals.

In this paper we focus on self calibration for sensor position errors. Rockah and Schultheiss [1] showed that simultaneous DOA estimation and sensor location calibration is possible provided that the array is not linear and that there are three distinct sources as well as knowledge of the exact location of one sensor and the direction to a second sensor. Existing self calibration techniques assume that calibration errors are small and use a first order approximation to the perturbed array response vector in their cost functions to simplify the estimation procedure. Our simulations indicate that a first order approximation to sensor location errors is not adequate as the errors increase [43]. In many applications, sensor perturbations can be larger than the small errors these techniques were designed to handle. In this paper, we combine portions of the techniques in [16], [31], [32], and [44] to construct a more robust procedure that does not use an approximation to sensor location errors. The development is based on an exact calibration procedure for known sources developed by Fistas and Manikas (FM) in [16] combined with a non-parametric steering vector estimation (SVE) technique from [44] for estimation of large calibration errors. This iterates with a modified noise subspace fitting (NSF) DOA estimation technique from [31] and [45], and final refinements are made using the WF self calibration technique [32].

This paper is organized as follows. The problem is formulated in Section 2. The FM calibration technique, the NSF DOA estimation technique, and the WF and MAP-NSF self calibration algorithms are summarized in Section 3. In Section 4, the SVE algorithm is summarized and the large error self calibration procedure is developed. Simulation results are presented in Section 5, and a summary is given in Section 6.

## 2 Problem Formulation

Our problem consists of $M$ narrowband radiating sources with center frequency $\omega_0$ being received by an array of $N$ sensors, where $M < N$. The signal at the output of the sensors can be described by the $N \times 1$ column vector

$$\mathbf{x}(t) = \boldsymbol{\mathcal{V}}(\boldsymbol{\phi}, \boldsymbol{\rho})\mathbf{s}(t) + \mathbf{n}(t), \tag{1}$$

where $\mathbf{n}(t)$ is the $N \times 1$ noise vector, $\mathbf{s}(t)$ is the $M \times 1$ vector of source signals, and $\boldsymbol{\mathcal{V}}(\boldsymbol{\phi}, \boldsymbol{\rho})$ is the $N \times M$ array response matrix.

The columns of $\boldsymbol{\mathcal{V}}(\boldsymbol{\phi}, \boldsymbol{\rho})$ are the array response vectors (also called steering vectors) for the individual sources,

$$\boldsymbol{\mathcal{V}}(\boldsymbol{\phi}, \boldsymbol{\rho}) = \left[\mathbf{V}(\phi_1, \boldsymbol{\rho})\ \mathbf{V}(\phi_2, \boldsymbol{\rho})\ \cdots\ \mathbf{V}(\phi_M, \boldsymbol{\rho})\right]. \tag{2}$$

The array response vectors are a function of the source DOAs $\boldsymbol{\phi}$ and the sensor parameters $\boldsymbol{\rho}$. In general, $\boldsymbol{\rho}$ consists of sensor positions, gain, phase, mutual coupling, etc. We initially consider only perturbations of the sensor positions, and assume the other parameters are known. The array response of the $n$th sensor to a source from $\phi_m$ is

$$V_n(\phi_m, \boldsymbol{\rho}) = \exp\left\{j\frac{2\pi}{\lambda}(x_n \cos\phi_m + y_n \sin\phi_m)\right\}, \tag{3}$$

where $x_n$ and $y_n$ are the $x$ and $y$ positions of the $n$th sensor and $\lambda$ is the wavelength corresponding to $\omega_0$.

We assume that the positions are perturbed from their nominal positions by $\Delta x_n$ and $\Delta y_n$. Let $\boldsymbol{\rho}_0$ denote the vector of nominal position parameters, and $\boldsymbol{\rho}_\Delta$ denote the perturbations. The perturbed array response has the form

$$V_n(\phi_m, \boldsymbol{\rho}_0 + \boldsymbol{\rho}_\Delta) = \exp\left\{j\frac{2\pi}{\lambda}\left[(x_n + \Delta x_n)\cos\phi_m + (y_n + \Delta y_n)\sin\phi_m\right]\right\}. \tag{4}$$

The perturbations are modeled as a zero-mean Gaussian random vector with covariance matrix $\boldsymbol{\Omega}$. The DOAs are assumed to be non-random parameters. The goal is to estimate the sensor position perturbations as well as the DOAs of the sources using $K$ independent data snapshots taken at times $t_1, \ldots, t_K$. Our primary goal is accurate DOA estimation, with perturbation parameters considered as nuisance parameters that must also be estimated.

The source signals and noise are assumed to be sample functions of uncorrelated zero-mean Gaussian random processes. The noise is uncorrelated from

sensor to sensor with noise power $\sigma^2$, thus the noise covariance matrix is given by

$$\mathbf{R}_n = E\{\mathbf{n}(t)\mathbf{n}(t)^H\} = \sigma^2\mathbf{I}_N, \tag{5}$$

where $\mathbf{I}_N$ is the $N \times N$ identity matrix. The source signals are uncorrelated with the noise and each other. Let $\sigma_m^2$ denote the power of the $m$th source. The source covariance matrix is the $M \times M$ diagonal matrix

$$\mathbf{R}_s = E\{\mathbf{s}(t)\mathbf{s}(t)^H\} = \mathrm{diag}\{\sigma_1^2, \ldots, \sigma_M^2\} = \begin{bmatrix} \sigma_1^2 & 0 & \cdots & 0 \\ 0 & \sigma_2^2 & \cdots & 0 \\ & & \ddots & \\ 0 & 0 & \cdots & \sigma_M^2 \end{bmatrix}. \tag{6}$$

The data covariance matrix $\mathbf{R}_\mathbf{x}$ has the form

$$\mathbf{R}_\mathbf{x} = E\left\{\mathbf{x}(t)\mathbf{x}(t)^H\right\} = \boldsymbol{\mathcal{V}}(\boldsymbol{\phi}, \boldsymbol{\rho})\mathbf{R}_s\boldsymbol{\mathcal{V}}(\boldsymbol{\phi}, \boldsymbol{\rho})^H + \sigma^2\mathbf{I}_N. \tag{7}$$

The techniques we will investigate rely heavily on the eigen-decomposition of $\mathbf{R}_\mathbf{x}$, which has the form

$$\mathbf{R}_\mathbf{x} = \mathbf{E}_s\boldsymbol{\Lambda}_s\mathbf{E}_s^H + \sigma^2\mathbf{E}_n\mathbf{E}_n^H, \tag{8}$$

where $\mathbf{E}_s$ is the $N \times M$ matrix of the signal subspace eigenvectors, $\boldsymbol{\Lambda}_s$ is a diagonal matrix containing the $M$ signal subspace eigenvalues, and $\mathbf{E}_n$ is the $N \times (N - M)$ matrix of the noise subspace eigenvectors which all have eigenvalue $\sigma^2$. The eigen-decomposition in (8) can be re-written as

$$\begin{aligned} \mathbf{R}_\mathbf{x} &= \mathbf{E}_s\left(\boldsymbol{\Lambda}_s - \sigma^2\mathbf{I}_M\right)\mathbf{E}_s^H + \sigma^2\mathbf{E}_s\mathbf{E}_s^H + \sigma^2\mathbf{E}_n\mathbf{E}_n^H \\ &= \mathbf{E}_s\left(\boldsymbol{\Lambda}_s - \sigma^2\mathbf{I}_M\right)\mathbf{E}_s^H + \sigma^2\mathbf{I}_N. \end{aligned} \tag{9}$$

Comparing (7) and (9), we have the relationship

$$\boldsymbol{\mathcal{V}}(\boldsymbol{\phi}, \boldsymbol{\rho})\mathbf{R}_s\boldsymbol{\mathcal{V}}(\boldsymbol{\phi}, \boldsymbol{\rho})^H = \mathbf{E}_s\left(\boldsymbol{\Lambda}_s - \sigma^2\mathbf{I}_M\right)\mathbf{E}_s^H. \tag{10}$$

This relationship establishes the well known fact that the array response vectors in $\boldsymbol{\mathcal{V}}(\boldsymbol{\phi}, \boldsymbol{\rho})$ and the signal subspace eigenvectors in $\mathbf{E}_s$ both span the signal subspace.

In practice, the eigenvectors and eigenvalues are estimated from the sample covariance matrix $\hat{\mathbf{R}}_{\mathbf{x}}$,

$$\hat{\mathbf{R}}_{\mathbf{x}} = \frac{1}{K}\sum_{k=1}^{K} \mathbf{x}(t_k)\mathbf{x}(t_k)^H = \hat{\mathbf{E}}_s \hat{\mathbf{\Lambda}}_s \hat{\mathbf{E}}_s^H + \hat{\sigma}^2 \hat{\mathbf{E}}_n \hat{\mathbf{E}}_n^H, \tag{11}$$

where the eigenvectors in $\hat{\mathbf{E}}_s$ and $\hat{\mathbf{E}}_n$ are obtained directly from the numerical eigen-decomposition of $\hat{\mathbf{R}}_{\mathbf{x}}$. The signal subspace eigenvalues in $\hat{\mathbf{\Lambda}}_s$ are the $M$ largest eigenvalues, and the noise power $\hat{\sigma}^2$ is estimated from the average of the $N - M$ smallest eigenvalues, e.g.

$$\hat{\sigma}^2 = \frac{1}{N-M}\sum_{i=M+1}^{N} \hat{\lambda}_i. \tag{12}$$

The Cramer-Rao bound (CRB) for the random signal model with non-random DOAs and random perturbations was developed in [30] for generic array perturbations. It is based on the hybrid CRB structure developed by Rockah and Schultheiss in [1] for combinations of random and non-random parameters. An explicit evaluation of the terms in the bound for position perturbations follows directly from [30] and is carried out in [43]. Using this bound, the identifiability conditions of a non-linear array, three distinct sources ($M \geq 3$), and knowledge of three components of the perturbation vector (e.g. the exact location of one sensor and the direction to a second sensor or the exact location of one sensor and the $x$-component of a second sensor) derived in [1] for a different signal model were also verified numerically in [43], and are assumed to be satisfied. Thus the perturbation vector $\boldsymbol{\rho}_\Delta$ will consist of the $L = 2N - 3$ unknown $x$ and $y$ components of the sensor perturbations.

The identifiability conditions guarantee that the CRB for the DOAs decreases as the signal-to-noise ratio (SNR) increases. This occurs in spite of the fact that the CRB for the perturbation parameters levels out and does not decrease beyond a fixed value related to the a priori variance when SNR increases [24].

## 3 Calibration Techniques

### *3.1 Array Calibration with Known DOAs*

If the DOAs and the array response vectors for two distinct sources are known, the sensor locations can be obtained exactly from the definition in (3). When there are also gain and phase uncertainties, all parameters can be found from

knowledge of the DOAs and array response vectors for three distinct sources. Fistas and Manikas have developed a technique for estimating the parameters from measured array response vectors when three sources are observed individually [16].

Given the array response matrix and the source DOAs, the sensor location estimation is based on the following relationships. Let $V_{1,n}$, $V_{2,n}$ and $V_{3,n}$ denote the response of the $n$th sensor to sources with DOAs $\phi_1$, $\phi_2$, and $\phi_3$, respectively. Then

$$V_{2,n}^* V_{1,n} = \exp\left\{ j\frac{2\pi}{\lambda}\left(x_n[\cos\phi_1 - \cos\phi_2] + y_n[\sin\phi_1 - \sin\phi_2]\right)\right\} \tag{13}$$

$$V_{3,n}^* V_{1,n} = \exp\left\{ j\frac{2\pi}{\lambda}\left(x_n[\cos\phi_1 - \cos\phi_3] + y_n[\sin\phi_1 - \sin\phi_3]\right)\right\}. \tag{14}$$

Rearranging these equations, the sensor positions can then be obtained in direct form using:

$$\begin{bmatrix} \hat{x}_n \\ \hat{y}_n \end{bmatrix} = \begin{bmatrix} x_n + \Delta\hat{x}_n \\ y_n + \Delta\hat{y}_n \end{bmatrix} = \begin{bmatrix} c_{12} & s_{12} \\ c_{13} & s_{13} \end{bmatrix}^{-1} \begin{bmatrix} \frac{\lambda}{2\pi}\angle(V_{2,n}^* V_{1,n}) \\ \frac{\lambda}{2\pi}\angle(V_{3,n}^* V_{1,n}) \end{bmatrix} \tag{15}$$

where $c_{12} = \cos\phi_1 - \cos\phi_2$, $c_{13} = \cos\phi_1 - \cos\phi_3$, $s_{12} = \sin\phi_1 - \sin\phi_2$, and $s_{13} = \sin\phi_1 - \sin\phi_3$. The function $\angle(\cdot)$ extracts the angle of a complex number, i.e. $\angle(re^{j\theta}) = \theta$.

In practice, the array response vectors are not known. However, when a source is observed individually, an unstructured estimate of its array response vector can be obtained from the sole signal subspace eigenvector of the sample covariance matrix. This technique is useful when a single known source can be observed from different DOAs. In many practical situations, however, this is not possible.

### *3.2 Small Perturbation Self Calibration Techniques*

In our problem formulation, we have modeled DOAs as non-random parameters and the sensor perturbations as random parameters. Our goal is to estimate the DOAs, with perturbation parameters considered as nuisance parameters that must be estimated simultaneously. Self calibration techniques jointly estimate the unknown sensor positions and the DOAs of interest for targets of opportunity. A number of techniques have been developed in which the sensor parameters are modeled as either non-random parameters or random parameters. Both types of techniques can be applied under our model. The techniques

for non-random parameters simply ignore the additional information provided by the a priori distribution of the random parameters.

Two techniques that we study in detail in this paper are the WF technique developed by Weiss and Friedlander [32] and the MAP-NSF technique developed by Viberg and Swindlehurst [31]. The WF technique assumes the perturbation vector $\boldsymbol{\rho}_\Delta$ is a non-random parameter vector. It is based on the MUSIC algorithm in which DOA estimates are obtained (assuming that sensor location parameters are known) from the positions of the $M$ largest peaks in the MUSIC "spectrum":

$$P_{MU}(\phi) = \left(\mathbf{V}(\phi,\boldsymbol{\rho})^H \hat{\mathbf{E}}_n \hat{\mathbf{E}}_n^H \mathbf{V}(\phi,\boldsymbol{\rho})\right)^{-1}, \tag{16}$$

or equivalently, from the peaks in the MUSIC cost function

$$C_{MU}(\phi) = \mathbf{V}(\phi,\boldsymbol{\rho})^H \hat{\mathbf{E}}_s \hat{\mathbf{E}}_s^H \mathbf{V}(\phi,\boldsymbol{\rho}). \tag{17}$$

Weiss and Friedlander suggested that if the source DOAs are known, the perturbation parameters could be obtained by maximizing the same cost function with respect to the perturbation parameters, summed over all the sources, i.e

$$C_{WF}(\boldsymbol{\rho}_\Delta) = \sum_{m=1}^{M} \mathbf{V}(\phi_m,\boldsymbol{\rho}_0+\boldsymbol{\rho}_\Delta)^H \hat{\mathbf{E}}_s \hat{\mathbf{E}}_s^H \mathbf{V}(\phi_m,\boldsymbol{\rho}_0+\boldsymbol{\rho}_\Delta). \tag{18}$$

This may be expressed compactly by defining $\mathbf{v}(\boldsymbol{\phi},\boldsymbol{\rho})$ to be the $NM \times 1$ column vector obtained by stacking the columns of $\boldsymbol{\mathcal{V}}(\boldsymbol{\phi},\boldsymbol{\rho})$, i.e.

$$\mathbf{v}(\boldsymbol{\phi},\boldsymbol{\rho}) = \mathrm{vec}(\boldsymbol{\mathcal{V}}(\boldsymbol{\phi},\boldsymbol{\rho})). \tag{19}$$

The cost function becomes

$$C_{WF}(\boldsymbol{\rho}_\Delta) = \mathbf{v}(\boldsymbol{\phi},\boldsymbol{\rho}_0+\boldsymbol{\rho}_\Delta)^H (\mathbf{I}_M \otimes \hat{\mathbf{E}}_s \hat{\mathbf{E}}_s^H) \mathbf{v}(\boldsymbol{\phi},\boldsymbol{\rho}_0+\boldsymbol{\rho}_\Delta), \tag{20}$$

where $\otimes$ denotes the Kronecker product. This is a complicated multi-dimensional optimization problem. However, if the location errors are small, the array steering vector can be modeled by the first order approximation

$$\mathbf{v}(\boldsymbol{\phi},\boldsymbol{\rho}_0+\boldsymbol{\rho}_\Delta) \approx \mathbf{v}_0 + \mathbf{D}_\rho \boldsymbol{\rho}_\Delta, \tag{21}$$

where $\mathbf{v}_0 = \mathrm{vec}(\boldsymbol{\mathcal{V}}(\boldsymbol{\phi},\boldsymbol{\rho}_0))$ and $\mathbf{D}_\rho$ is the $NM \times L$ derivative matrix

$$\mathbf{D}_\rho = \left[\frac{\partial \mathbf{v}(\boldsymbol{\phi},\boldsymbol{\rho})}{\partial \rho_1} \;\cdots\; \frac{\partial \mathbf{v}(\boldsymbol{\phi},\boldsymbol{\rho})}{\partial \rho_L}\right]\Bigg|_{\boldsymbol{\rho}=\boldsymbol{\rho}_0}. \tag{22}$$

The cost function becomes

$$C_{WF}(\boldsymbol{\rho}_\Delta) = (\mathbf{v}_0 + \mathbf{D}_\rho \boldsymbol{\rho}_\Delta)^H (\mathbf{I}_M \otimes \hat{\mathbf{E}}_s \hat{\mathbf{E}}_s^H)(\mathbf{v}_0 + \mathbf{D}_\rho \boldsymbol{\rho}_\Delta). \tag{23}$$

Defining

$$\boldsymbol{\Gamma}_{WF} = \mathrm{Re}\left\{ \mathbf{D}_\rho^H \left( \mathbf{I}_M \otimes \left[ \hat{\mathbf{E}}_s \hat{\mathbf{E}}_s^H \right] \right) \mathbf{D}_\rho \right\} \tag{24}$$

and

$$\mathbf{f}_{WF} = \mathrm{Re}\left\{ \mathbf{D}_\rho^H \left( \mathbf{I}_M \otimes \left[ \hat{\mathbf{E}}_s \hat{\mathbf{E}}_s^H \right] \right) \mathbf{v}_0 \right\}, \tag{25}$$

the solution to this optimization problem is

$$\hat{\boldsymbol{\rho}}_\Delta = -\boldsymbol{\Gamma}_{WF}^{-1} \mathbf{f}_{WF}. \tag{26}$$

The combined DOA estimation and sensor position calibration algorithm consists of estimating the DOAs using (17), then using the DOA estimates to estimate the location errors using (26). The algorithm iterates until it converges to a final solution. The WF technique requires initial DOA estimates, which may be obtained from the MUSIC algorithm using the nominal sensor positions.

The MAP-NSF algorithm was developed to solve the gain/phase calibration problem, but is easily adapted to the location error problem. It is based on the NSF DOA estimation algorithm [45] in which DOA estimates are obtained (assuming that sensor location parameters are known) from an $M$-dimensional maximization of the NSF cost function

$$C_{NSF}(\boldsymbol{\phi}) = \mathbf{v}(\boldsymbol{\phi}, \boldsymbol{\rho})^H \hat{\mathbf{W}} \mathbf{v}(\boldsymbol{\phi}, \boldsymbol{\rho}) \tag{27}$$

where

$$\hat{\mathbf{W}} = \hat{\sigma}^{-2} \left( \left[ \hat{\boldsymbol{\mathcal{V}}}^{\uparrow} \hat{\mathbf{E}}_s \left( \hat{\boldsymbol{\Lambda}}_s - \hat{\sigma}^2 \mathbf{I}_M \right)^2 \hat{\boldsymbol{\Lambda}}_s^{-1} \hat{\mathbf{E}}_s^H \hat{\boldsymbol{\mathcal{V}}}^{\uparrow H} \right]^T \otimes \left[ \hat{\mathbf{E}}_n \hat{\mathbf{E}}_n^H \right] \right), \tag{28}$$

and

$$\hat{\boldsymbol{\mathcal{V}}}^{\uparrow} = \left( \hat{\boldsymbol{\mathcal{V}}}^H \hat{\boldsymbol{\mathcal{V}}} \right)^{-1} \hat{\boldsymbol{\mathcal{V}}}^H. \tag{29}$$

The matrix $\hat{\boldsymbol{\mathcal{V}}} = \boldsymbol{\mathcal{V}}(\hat{\boldsymbol{\phi}}, \boldsymbol{\rho})$ is an estimate of the array response matrix from some initial DOA estimates and the known array parameters. The remaining

quantities in (28) are obtained from the eigen-decomposition of the sample covariance matrix in (11).

In the MAP-NSF technique, the perturbation vector $\boldsymbol{\rho}_\Delta$ is assumed to be a zero-mean Gaussian random vector with covariance matrix $\boldsymbol{\Omega}$, and the DOAs and perturbation parameters are estimated jointly using a maximum a posteriori (MAP) approach. The first order approximation to the perturbed array response vector given in (21) is used, and the following cost function is obtained:

$$C_{MAP-NSF}(\boldsymbol{\phi}, \boldsymbol{\rho}_\Delta) = (\mathbf{v}_0 + \mathbf{D}_\rho \boldsymbol{\rho}_\Delta)^H \hat{\mathbf{W}} (\mathbf{v}_0 + \mathbf{D}_\rho \boldsymbol{\rho}_\Delta) + \frac{1}{2} \boldsymbol{\rho}_\Delta^T \boldsymbol{\Omega}^{-1} \boldsymbol{\rho}_\Delta \quad (30)$$

where $\hat{\mathbf{W}}$ is defined in (28) and $\hat{\boldsymbol{\mathcal{V}}} = \boldsymbol{\mathcal{V}}(\hat{\boldsymbol{\phi}}, \boldsymbol{\rho}_0)$ is an estimate of the array response matrix from some initial DOA estimates and the nominal array parameters. Defining

$$\boldsymbol{\Gamma}_{MAP} = \mathrm{Re}\left\{ \mathbf{D}_\rho^H \hat{\mathbf{W}} \mathbf{D}_\rho + \frac{1}{2} \boldsymbol{\Omega}^{-1} \right\} \quad (31)$$

$$\mathbf{f}_{MAP} = \mathrm{Re}\left\{ \mathbf{D}_\rho^H \hat{\mathbf{W}} \mathbf{v}_0 \right\}, \quad (32)$$

we obtain an estimate of the perturbation parameters from

$$\hat{\boldsymbol{\rho}}_\Delta = -\boldsymbol{\Gamma}_{MAP}^{-1} \mathbf{f}_{MAP}. \quad (33)$$

This can be plugged back into (30) and the DOA estimates can be obtained from the resulting composite cost function

$$C_{MAP-NSF}(\boldsymbol{\phi}) = \mathbf{v}_0^H \hat{\mathbf{W}} \mathbf{v}_0 - \mathbf{f}_{MAP}^T \boldsymbol{\Gamma}_{MAP}^{-1} \mathbf{f}_{MAP} \quad (34)$$

where $\mathbf{v}_0$, $\mathbf{f}_{MAP}$ and $\boldsymbol{\Gamma}_{MAP}$ are all functions of $\boldsymbol{\phi}$. MAP-NSF requires initial DOA estimates and knowledge of the perturbation covariance matrix $\boldsymbol{\Omega}$. MAP-NSF is not an iterative technique, but requires finding the maximum of an $M$-dimensional cost function.

The performance of the WF and MAP-NSF algorithms was simulated and the results are shown in Figure 1. A 6 element circular array with $\lambda/2$ spacing was used. The signals impinging on the array were at azimuth angles of 37.3, 0.0, and -37.3 degrees. All three signals are just within the null-to-null beamwidth of the array. The signals were uncorrelated with equal power. In order to satisfy the identifiability conditions, the exact location of one sensor, and the $x$ position of a second sensor were assumed known. The perturbations for the remaining sensor locations were modeled as independent, identically distributed Gaussian random variables in both the $x$ and $y$ directions with

standard deviations varying from 0 to 0.15 $\lambda$. In all cases, $K = 1000$ snapshots of data were collected and the results were averaged over 200 trials. The sensor location perturbations were constant over the 1000 snapshots for each trial, but varied from trial to trial according to their a priori Gaussian distributions. The mean square error of the DOA estimate for the first signal vs. SNR is shown in each plot, where the SNR is defined as the ratio of the signal power to the noise power $\sigma_1^2/\sigma^2$. The DOA estimation results for the other signals are comparable.

MAP-NSF was initialized using an alternating minimization technique and nominal sensor positions. First only one signal is assumed present and the MAP-NSF cost function is minimized with respect to it's DOA. The resulting DOA estimate is then held fixed and the MAP-NSF function assuming two source signals is minimized with respect to the second DOA. This method is repeated for as many source signals as are present.

WF was initialized with DOA estimates obtained from the standard MUSIC algorithm assuming nominal sensor positions (WF(MUSIC)). MAP-NSF performs better than the standard MUSIC algorithm when there are position perturbations, but WF shows almost no improvement. With better initialization, however, WF generally has better performance than MAP-NSF [43]. To demonstrate this, we also show results obtained with the WF technique initialized by the true DOAs (WF(True)), and by the estimates obtained from MAP-NSF (WF(MAP-NSF)). We see that much better results are obtained with more accurate initial DOA estimates. All algorithms deviate significantly from the Cramer-Rao bound as the sensor location perturbations increase. The poor performance is due to the failure of the small error assumption in (21).

Since it is not fair to initialize with the true DOAs, for the remainder of this paper, WF is initialized with MAP-NSF. This can also be viewed as post-processing MAP-NSF with WF. We refer to this procedure as MAP-NSF/WF.

## 4 DOA Estimation and Large Sensor Position Perturbation Calibration

The results in the previous section indicate that a first order approximation to sensor location errors is not adequate as the errors increase. A second order model may be appropriate, but we would ideally like to use an exact solution for the sensor locations, such as in [16].

In our problem, there are three or more sources present simultaneously, and the array response vectors cannot be individually observed so the technique in [16] cannot be applied directly. However, there are techniques for obtaining

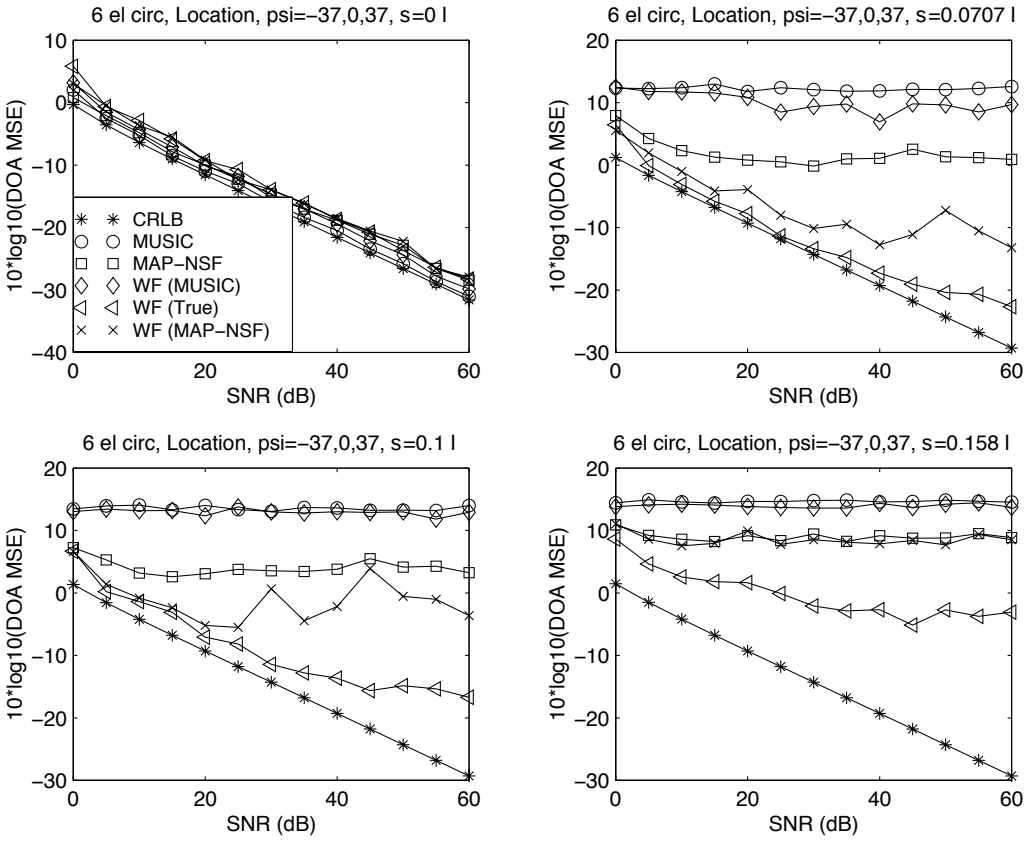


Fig. 1. Comparison of DOA estimation performance vs. SNR for random sensor location perturbations with standard deviation ranging from 0 to 0.15 $\lambda$. The array is a 6 element half-wavelength spaced uniform circular array. There are 3 equal power uncorrelated sources impinging on the array with DOAs of -37.3, 0.0, and 37.3 degrees. Number of snapshots was 1000. The results were averaged over 200 trials.

unstructured steering vector estimates from the sample covariance matrix. Examples are the PROS algorithm developed by Tseng, Feldman, and Griffiths [46] and a technique based on second order moments developed by Weiss and Friedlander [44], herein referred to as the steering vector estimation (SVE) algorithm.

In the SVE algorithm, the $N \times M$ array response vector matrix $\boldsymbol{\mathcal{V}}$ is assumed to have an unstructured form where the $n, m$ element has a real gain $g_n$ and phase angle $\theta_{n,m}$, i.e. $V_{n,m} = g_n e^{j\theta_{n,m}}$. The matrix $\boldsymbol{\mathcal{V}}$ can be written as

$$\boldsymbol{\mathcal{V}} = \mathbf{GC} \tag{35}$$

where $\mathbf{G}$ is an $N \times N$ diagonal matrix of real sensor gains, $\mathbf{G} = \text{diag}\{g_1, g_2, \ldots, g_N\}$, and $\mathbf{C}$ is an $N \times M$ matrix of unit magnitude complex phase responses, i.e. $C_{n,m} = e^{j\theta_{n,m}}$. The steering vectors can only be determined up to a complex

scale factor, therefore it is assumed without loss of generality that the first element of each vector is equal to one, i.e. $g_1 = 1$ and $\theta_{1,1} = \cdots = \theta_{1,M} = 0$.

The algorithm is based on the relationship between the parametric model and the eigen-decomposition model of the signal subspace in (10). An equivalent relationship is

$$\boldsymbol{\mathcal{V}}\mathbf{R}_s^{1/2} = \mathbf{E}_s \left(\boldsymbol{\Lambda}_s - \sigma^2 \mathbf{I}_M\right)^{1/2} \mathbf{S}, \tag{36}$$

where $\mathbf{S}$ is any $M \times M$ orthonormal matrix. (We can obtain (10) from (36) by post-multiplying each side by its hermitian transpose.) Defining

$$\mathbf{B} = \mathbf{E}_s \left(\boldsymbol{\Lambda}_s - \sigma^2 \mathbf{I}_M\right)^{1/2} \tag{37}$$

and substituting (35) and (37) into (36), we have

$$\mathbf{G}\mathbf{C}\mathbf{R}_s^{1/2} = \mathbf{B}\mathbf{S}. \tag{38}$$

Let $\hat{\mathbf{B}} = \hat{\mathbf{E}}_s \left(\hat{\boldsymbol{\Lambda}}_s - \hat{\sigma}^2 \mathbf{I}_M\right)^{1/2}$ be an estimate of $\mathbf{B}$ obtained by substituting the estimates $\hat{\mathbf{E}}_s$, $\hat{\boldsymbol{\Lambda}}_s$, and $\hat{\sigma}^2$ in the right hand side of (37). The SVE algorithm obtains estimates of the matrices $\mathbf{G}, \mathbf{C}, \mathbf{R}_s^{1/2}$, and $\mathbf{S}$ by replacing $\mathbf{B}$ with $\hat{\mathbf{B}}$ and minimizing the $L_2$-norm of the difference between the right and left hand sides of (38), i.e. it minimizes the cost function

$$Z = \left\| \mathbf{G}\mathbf{C}\mathbf{R}_s^{1/2} - \hat{\mathbf{B}}\mathbf{S} \right\|^2. \tag{39}$$

At each step of algorithm, the matrices $\mathbf{G}$, $\mathbf{C}$, $\mathbf{R}_s^{1/2}$, and $\mathbf{S}$ are estimated separately by holding all of the other matrices fixed. Note that $\mathbf{G}$ and $\mathbf{R}_s^{1/2} = \text{diag}\{\sigma_1, \ldots, \sigma_M\}$ are diagonal matrices. Details of the algorithm are available in [44], and summarized here:

(1) $\hat{\mathbf{S}} = \mathbf{U}\mathbf{H}^H$, where $\mathbf{U}\boldsymbol{\Sigma}\mathbf{H}$ is the singular value decomposition of $\hat{\mathbf{B}}^H \hat{\mathbf{G}}\hat{\mathbf{C}}\hat{\mathbf{R}}_s^{1/2}$.

(2) $\hat{g}_n = \max\left(0, \text{Re}\left\{\left[\hat{\mathbf{C}}\hat{\mathbf{R}}_s^{1/2}\right]_{(m)} \left[\hat{\mathbf{B}}\hat{\mathbf{S}}\right]_{(m)}^H\right\} / \| \left[\hat{\mathbf{C}}\hat{\mathbf{R}}_s^{1/2}\right]_{(m)} \|^2\right)$, $n = 2, \ldots, N$; where $[\cdot]_{(m)}$ denotes the $m$th row of a matrix.

(3) $\hat{\sigma}_m = \max\left(0, \text{Re}\left\{\left[\hat{\mathbf{G}}\hat{\mathbf{C}}\right]^{(n)H} \left[\hat{\mathbf{B}}\hat{\mathbf{S}}\right]^{(n)}\right\} / \| \left[\hat{\mathbf{G}}\hat{\mathbf{C}}\right]^{(n)} \|^2\right)$, $m = 1, \ldots, M$; where $[\cdot]^{(n)}$ denotes the $n$th column of a matrix.

(4) $\hat{C}_{mn} = \exp\left\{\angle[\hat{\mathbf{B}}\hat{\mathbf{S}}]_{m,n}\right\}$, $m = 1, \ldots, M$, $n = 2, \ldots, N$.

The algorithm iterates until convergence is achieved. The final unstructured array response matrix estimate is $\hat{\boldsymbol{\mathcal{V}}} = \hat{\mathbf{G}}\hat{\mathbf{C}}$.

Using the SVE algorithm with the FM technique, we can obtain sensor location estimates given knowledge of the source DOAs without using the small error approximation. The calibration process can then be coupled with a DOA estimation technique in an iterative procedure which alternates between DOA and array location estimation.

The MAP-NSF algorithm, which is based on the NSF cost function, is generally more robust to initialization errors and correlated sources than the WF algorithm, which is based on the MUSIC cost function. For these reasons, we use the NSF cost function as the basis for our DOA estimator. The DOA estimates are obtained by minimizing

$$Q(\boldsymbol{\phi}) = \mathbf{v}(\boldsymbol{\phi}, \boldsymbol{\rho})^H \hat{\mathbf{W}}_Q \mathbf{v}(\boldsymbol{\phi}, \boldsymbol{\rho}) \tag{40}$$

where $\hat{\mathbf{W}}_Q$ is the NSF matrix given in (28) but with the unstructured $\hat{\boldsymbol{\mathcal{V}}}$ obtained from the SVE algorithm. (In [47] we used the PROS algorithm for steering vector estimation but we have since found the SVE algorithm to provide better results [48],[43].) At each step of the minimization of (40) we use (15) to update our estimates of the sensor locations.

To summarize, this technique (denoted as 'Q') consists of the following steps:

(1) Initialization
   (a) Estimate the array manifold vectors, $\hat{\boldsymbol{\mathcal{V}}} = \hat{\mathbf{G}}\hat{\mathbf{C}}$, using the SVE algorithm [44], outlined above.
   (b) Obtain initial DOA estimates assuming nominal sensor positions and alternating minimization of the NSF cost function.
(2) Iterate on DOA and sensor position estimation
   (a) Estimate the sensor positions using the Fistas and Manikas sensor position estimation technique (15) with the unstructured estimate $\hat{\boldsymbol{\mathcal{V}}} = \hat{\mathbf{G}}\hat{\mathbf{C}}$ and the current DOA estimates.
   (b) Estimate the DOAs using the current sensor position estimates the large error SVE-NSF cost function (40).

The Q technique provides improved performance over the MAP-NSF and MAP-NSF/WF techniques for moderate to large perturbations as shown in the simulation results in Figure 2. However, the performance does not improve with increasing SNR, and never reaches the Cramer-Rao bound.

This technique does, however, give us considerably better estimates of the DOAs and the true sensor locations than we started with. The remaining sensor position deviations are small enough that the first order approximation used in WF and MAP-NSF is valid, and the DOA estimates are accurate enough for initialization of the WF technique. If we now apply WF, we see significant improvement for both small and large errors. This combined tech-

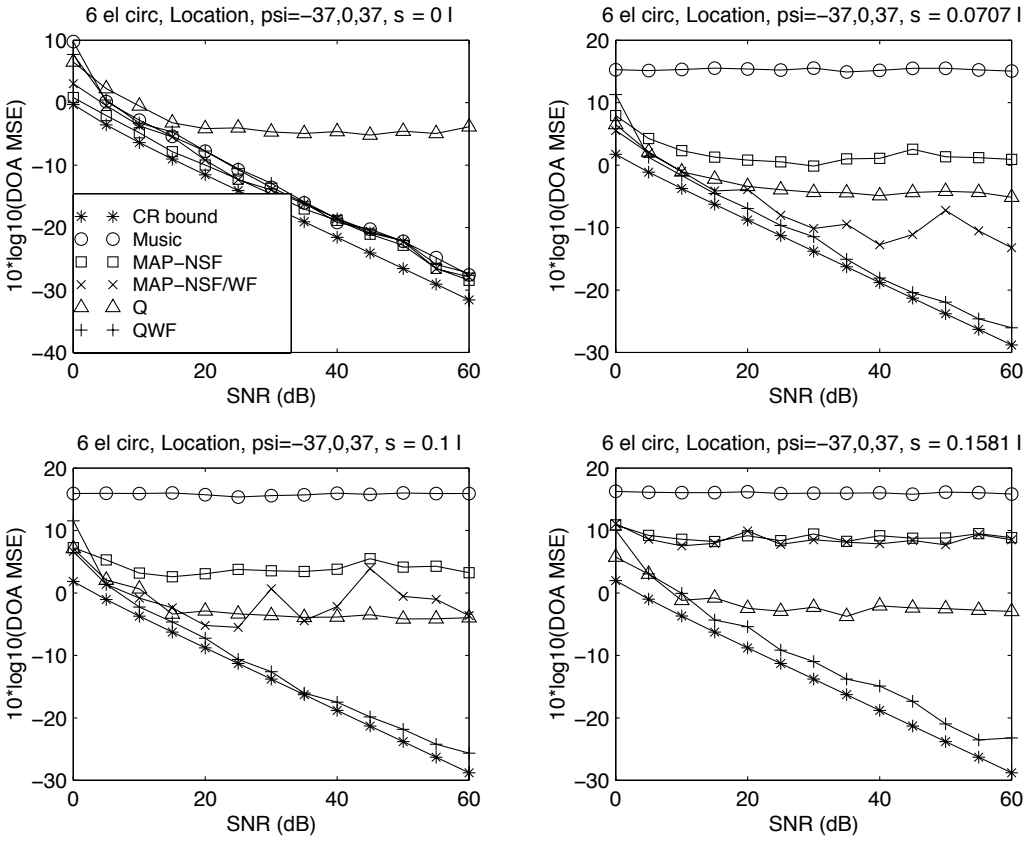


Fig. 2. Comparison of DOA estimation performance vs. SNR for random sensor location perturbations with standard deviation ranging from 0 to 0.15 $\lambda$. The array is a 6 element half-wavelength spaced uniform circular array. There are 3 equal power uncorrelated sources impinging on the array with DOAs of -37.3, 0.0, and 37.3 degrees. Number of snapshots was 1000. The results were averaged over 200 trials.

nique ('Q' followed by the WF algorithm) is referred to as the QWF technique. To summarize, the QWF technique consists of the following steps:

(1) Initialization : same as in Q technique
(2) Iterate on DOA and sensor position estimation as in Q technique
(3) Refine estimates using WF technique

The QWF procedure as stated above is the main result of this paper.

## 5 Simulation Results

DOA estimation performance and the Cramer-Rao bound are shown vs. SNR in Figure 2. The simulation scenario is the same as in Figure 1. A 6 element

circular array with $\lambda/2$ spacing was used. The signals impinging on the array were at azimuth angles of 37.3, 0.0, and -37.3 degrees. The signals were uncorrelated with equal power. In order to satisfy the identifiability conditions, the exact location of one sensor, and the $x$ position of a second sensor were assumed known. The perturbations for the remaining sensor locations were modeled as independent, identically distributed Gaussian random variables in both the $x$ and $y$ directions with standard deviations varying from 0 to 0.15 $\lambda$. In all cases, $K = 1000$ snapshots of data were collected and the results were averaged over 200 trials. The sensor location perturbations were constant over the 1000 snapshots for each trial, but varied from trial to trial according to their a priori Gaussian distributions. The mean square error of the DOA estimate for the first signal vs. SNR is shown in each plot.

Performance is compared to the standard MUSIC algorithm, the MAP-NSF self-calibration technique, and MAP-NSF followed by WF (MAP-NSF/WF). When there are no sensor perturbations, MUSIC is closest to the CRB, while all the others except the Q-function are close. Standard MUSIC fails immediately even for very small location errors. MAP-NSF provides a performance improvement over MUSIC but never reaches the bound. MAP-NSF/WF does reach the bound for small perturbation errors, but rapidly degrades as errors increase. The Q-function technique performs better than both MAP-NSF and MAP-NSF/WF only for moderate and large perturbations. The combined QWF technique provides the best performance over the range of sensor perturbations. Its performance gradually deviates from the CRB with increasing perturbation variance, but still has excellent performance at perturbation standard deviations as large as $0.158\lambda$.

DOA estimation performance and the CRB are shown vs. SNR and source separation for all the algorithms in Figures 3 and 4. The same 6 element circular array with $\lambda/2$ spacing was used. The three signals impinging on the array were at azimuth angle separations of 37, 27, and 17 degrees. The most closely spaced sources are well within the half-power beamwidth of the array. The sensor location perturbations, the number of snapshots, and the number of trials are all the same as in the first experiment. The QWF algorithm reaches the bound over the entire range of sensor perturbations and source DOA separations. Its performance gradually deviates from the CRB with increasing perturbation variance, but still has excellent performance at perturbation standard deviations as large as $0.158\lambda$ and source separations of only 17 degrees.

DOA estimation performance and the CRB are shown vs. the standard deviation of the location perturbations for all the algorithms in Figure 5. The same 6 element circular array with $\lambda/2$ spacing was used. The three signals impinging on the array were at azimuth angle separations of 37 degrees. The sensor location perturbations, the number of snapshots, and the number of

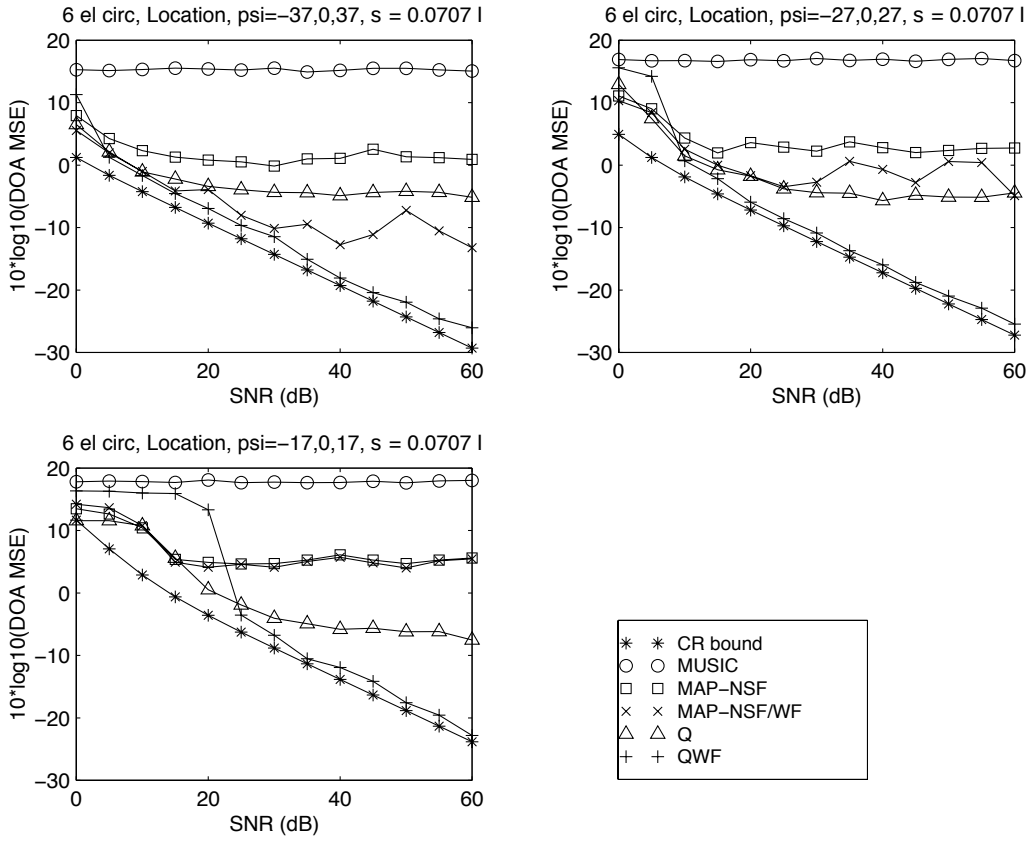


Fig. 3. Comparison of DOA estimation performance vs. SNR and source separation for random sensor location perturbations with standard deviation of 0.0707 $\lambda$. The array is a 6 element half-wavelength spaced uniform circular array. There are 3 equal power uncorrelated sources impinging on the array with source separations of 37, 27 and 17 degrees. Number of snapshots was 1000. The results were averaged over 200 trials.

trials are all the same as in the first experiment. The QWF algorithm comes closest to the bound over the entire range of sensor perturbations and SNRs. Its performance gradually deviates from the CRB with increasing perturbation variance, but still has excellent performance at perturbation standard deviations as large as $0.2\lambda$.

## 6 Summary

We considered the problem of array self calibration and showed the limitations of existing array self calibration algorithms against all but the smallest array element location errors. We then developed a more robust technique for calibration of large sensor perturbation errors which eliminates the small error approximation. The performance was compared to other techniques via

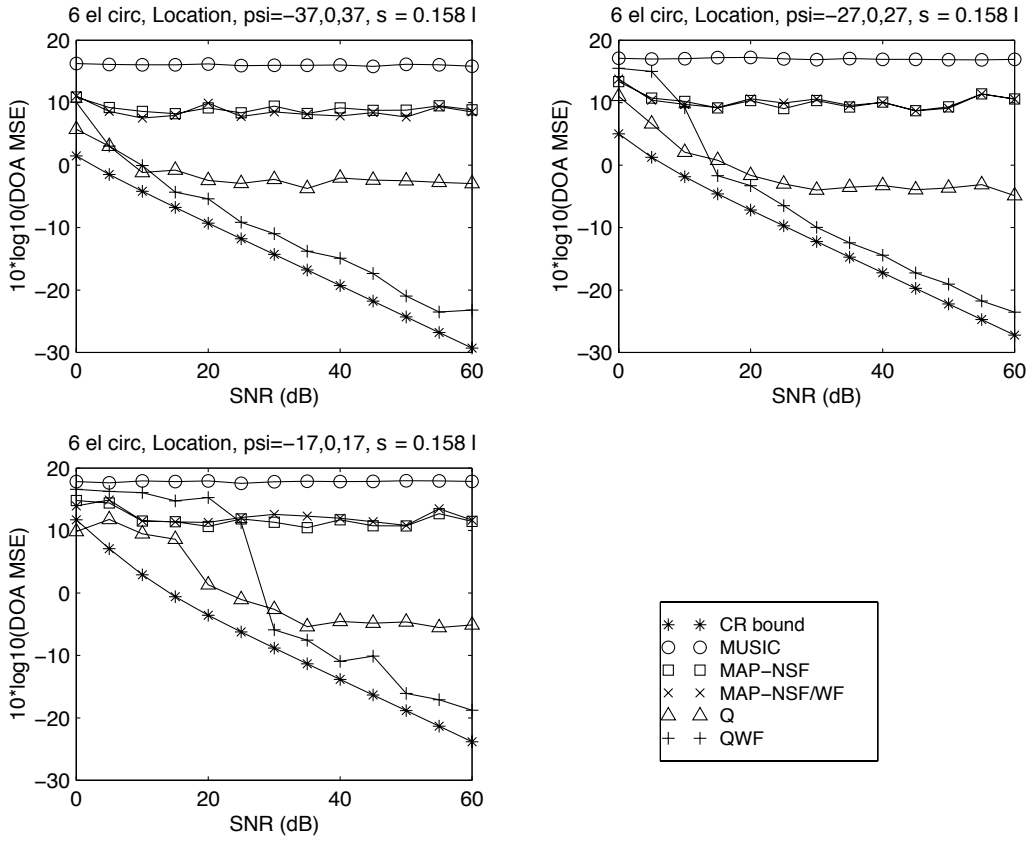


Fig. 4. Comparison of DOA estimation performance vs. SNR and source separation for random sensor location perturbations with standard deviation of 0.158 $\lambda$. The array is a 6 element half-wavelength spaced uniform circular array. There are 3 equal power uncorrelated sources impinging on the array with source separations of 37, 27 and 17 degrees. Number of snapshots was 1000. The results were averaged over 200 trials.

simulation. The QWF algorithm combines ideas from several existing techniques. It is able to make use of the best parts of these techniques to provide significantly improved performance over a wide range of sensor perturbation errors.

The QWF algorithm was designed specifically for sensor position errors. An extension to handle gain and phase perturbations when the sensor positions are known, as well as simultaneous sensor position, gain, and phase perturbations was also developed. It is described and analyzed via simulations in [43].

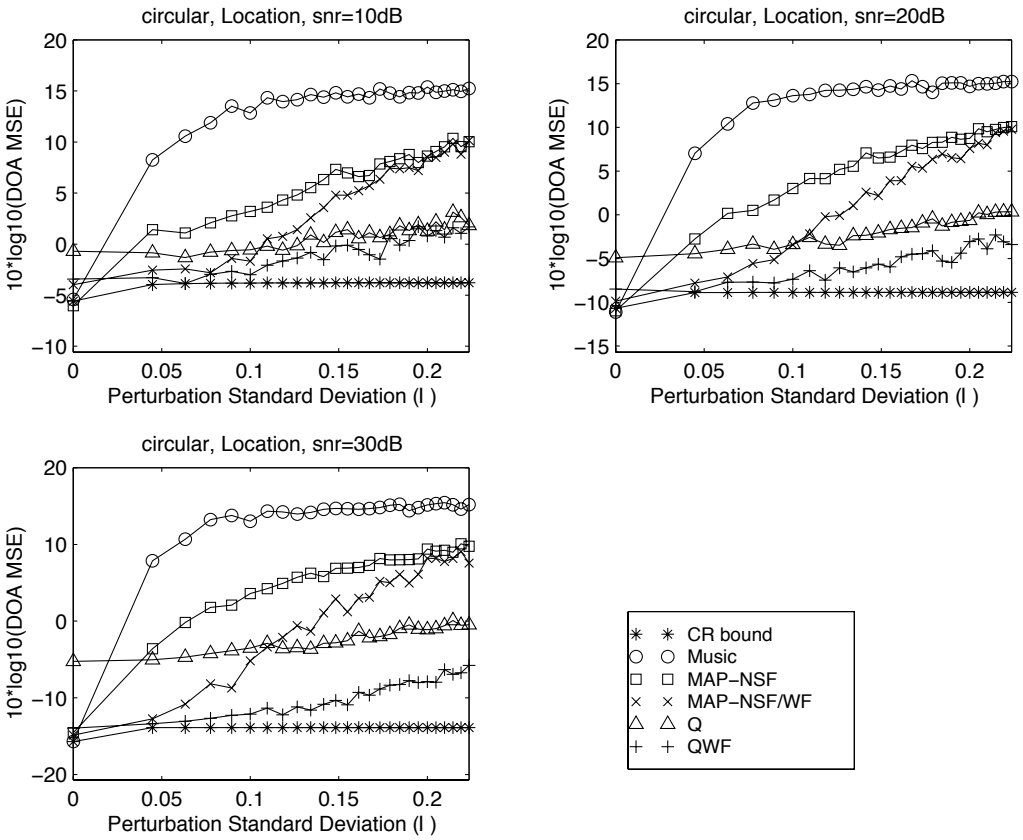


Fig. 5. Comparison of DOA estimation performance vs. standard deviation of sensor location perturbations for three different SNRs. The array is a 6 element half-wavelength spaced uniform circular array. There are 3 equal power uncorrelated sources impinging on the array with source separations of 37 degrees. Number of snapshots was 1000. The results were averaged over 200 trials.

## References

[1] Y. Rockah and P. M. Schultheiss, "Array Shape Calibration Using Sources in Unknown Locations - Part I: Far-Field Sources," *IEEE Trans. Acoustics, Speech, Signal Processing*, vol. 35, pp. 286-299, Mar. 1987.

[2] Y. Rockah, H. Messer, and P. M. Schultheiss, "Localization Performance of Arrays Subject to Phase Errors," *IEEE Trans. Aero. Elect. Syst.*, vol. 24, no. 4, pp. 402-410, July 1988.

[3] A.J. Weiss and B. Friedlander, "Self-Calibration for High-Resolution Array Processing," in *Advances in Spectrum and Array Processing, Vol. II*, (S. Haykin, Ed.), Ch. 10, Englewood Cliffs, NJ: Prentice-Hall, 1991.

[4] A.L. Swindlehurst and T. Kailath, "A Performance Analysis of Subspace-Based Methods in the Presence of Model Errors, Part I: The MUSIC Algorithm," *IEEE Trans. Signal Processing*, vol. 40, no. 7, pp. 1758-1773, July 1992.

[5] A.L. Swindlehurst and T. Kailath, "A Performance Analysis of Subspace-Based Methods in the Presence of Model Errors: Part II: Multidimensional Algorithms," *IEEE Trans. Signal Processing*, vol. 41, no. 9, pp. 2882-2890, Sept. 1993.

[6] M. Viberg and A. L. Swindlehurst, "Analysis of the Combined Effects of Finite Samples and Model Errors on Array Processing Performance," *IEEE Trans. Signal Processing*, vol. 42, no. 11, pp. 3073-3083, Nov. 1994.

[7] A. Ng, "Direction-of-Arrival Estimates in the Presence of Wavelength, Gain, and Phase Errors," *IEEE Trans. Signal Processing*, vol. 43, no. 1, pp. 225-232, Jan. 1995.

[8] R. Hamza and K. Buckley, "An Analysis of Weighted Eigenspace Methods in the Presence of Sensor Errors," *IEEE Trans. Signal Processing*, vol. 43, no.5, pp. 1140-1150, May 1995.

[9] T. Svantesson, "The Effects of Mutual Coupling Using a Linear Array of Thin Dipoles of Finite Length," *Proc. 9th IEEE Signal Processing Workshop on Statistical Signal and Array Processing*, pp. 232-235, 1998.

[10] Y. Rockah and P. M. Schultheiss, "Array Shape Calibration Using Sources in Unknown Locations - Part II: Near-field Sources and Estimator Implementation," *IEEE Trans. Acoustics, Speech, Signal Processing*, vol. 35, pp. 724-735, Jun. 1987.

[11] D. Fuhrmann, "Estimation of Sensor Gain and Phase Using Known Field Covariance," *Proc. of IEEE ICASSP 1991*, vol. 2, pp. 1369-1372, 1991.

[12] J. Clements and J. Lo, "Recursive Direction Finding in the Presence of Sensor Array Uncertainties," *Proc. of IEEE ICASSP 1993*, vol. 4, pp. 308-311, 1993.

[13] S. Talwar, A.Paulraj, G.H.Golub, "A Robust Numerical Approach for Array Calibration," *Proc. of IEEE ICASSP 1993*, vol. 4, pp. 316-319, 1993.

[14] D. Fuhrmann, "Estimation of Sensor Gain and Phase," *IEEE Trans. Signal Processing*, vol. 42, no. 1, pp. 77-87, Jan. 1994.

[15] B. Ng, M. Er, and C. Kot, "Array Gain/Phase Calibration Techniques for Adaptive Beamforming and Direction Finding," *IEE Proc. On Radar, Sonar, and Navigation*, vol. 141, no. 1, pp. 25-29, Feb. 1994.

[16] N. Fistas and A. Manikas, "A New General Global Array Calibration Method," *Proc. of IEEE ICASSP 1994*, vol. 4, pp. 73-76, 1994.

[17] A. Manikas and N. Fistas, "Modeling and Estimation of Mutual Coupling between Array Elements," *Proc. of IEEE ICASSP 1994*, vol. 4, pp. 553-556, 1994.

[18] F. McCarthy, R. Ridgway, A. Paulraj, "Fast Techniques for Sensor Array Calibration," *Proc. of 28th Asilomar Conf. On Sig., Syst., and Comp.*, pp. 688-693, 1994.

[19] B.C. Ng, C.M.Samson See, "Sensor-Array Calibration Using a Maximum-Likelihood Approach", *IEEE Trans. Antennas and Propagation*, vol. 44, no. 6, pp. 827-835, June 1996.

[20] J. Smith, Y. Leung, A. Cantoni, "Broadband Eigenvector Methods for Towed Array Shape Estimation with a Single Source," *Proc. of IEEE ICASSP 1996* vol. 6, pp. 3193-3196, 1996.

[21] C.M.Samson See, B.K.Poh, C.F.N.Cowan, "Sensor Array Calibration Using Measured Steering Vectors of Uncertain Location," *Proc. of IEEE ICASSP 1997*, vol. 5, pp. 3749-3752, 1997

[22] A. Manikas and C. Proukakis, "Modeling and Estimation of Ambiguities in Linear Arrays," *IEEE Trans. Signal Processing*, vol. 46, no. 8, pp. 2166-2179, Aug. 1998.

[23] M. Jansson, A.L. Swindlehurst, B. Ottersten, "Weighted Subspace Fitting for General Array Error Models," *IEEE Trans. Signal Processing*, vol. 46, no. 9, pp. 2484-2498, Sept. 1998.

[24] J. X. Zhu and H. Wang, "Effects of Sensor Position and Pattern Perturbations on CRLB for Direction Finding of Multiple Narrow-Band Sources," *Proc. of 4th Annual ASSP Workshop on Spectrum Estimation and Modeling*, pp. 98-102, 1988.

[25] J. Pierre, M. Kaveh, "Experimental Performance of Calibration and Direction Finding Algorithms," *Proc. of IEEE ICASSP 1991*, vol. 2, pp. 1365-1368, 1991.

[26] E. Hung, "A Critical Study of a Self-Calibrating Direction-Finding Method for Arrays," *IEEE Trans. Signal Processing*, vol. 42, no. 2, pp. 471-474, Feb. 1994.

[27] V.C. Soon, L. Tong, Y.F. Huang, R. Liu, "A Subspace Method for Estimating Sensor Gains and Phases," *IEEE Trans. Signal Processing*, vol. 42, no. 4, pp. 973-976, April 1994.

[28] M. Wylie, S. Roy, H. Messer, "Joint DOA Estimation and Phase Calibration of Linear Equispaced (LES) Arrays," *IEEE Trans. Signal Processing*, vol. 42, no. 12, pp. 3449-3459, Dec. 1994

[29] M. Zhang and Z. Zhu, "A Method for Direction Finding Under Sensor Gain and Phase Uncertainties," *IEEE Trans. Antennas and Propagation*, vol. 43, no. 8, pp. 880-883, Aug. 1995.

[30] B. Wahlberg, B. Ottersten, and M. Viberg, "Robust Signal Parameter Estimation in the Presence of Array Perturbations," *Proc. of IEEE ICASSP 1991*, pp. 3277-3280, 1991.

[31] M.Viberg and A.L.Swindlehurst, "A Bayesian Approach to Auto-Calibration for Parametric Array Signal Processing," *IEEE Trans. Signal Processing*, vol. 42, no. 12, pp. 3495-3507, Dec. 1994.

[32] A.J. Weiss and B. Friedlander, "Array Shape Calibration using Eigenstructure Methods," *Signal Processing*, vol. 22, no. 3, pp. 251-258, Elsevier Science Publishers, 1991.

[33] S. Hwang and D. Williams, "A Constrained Total Least Squares Approach for Sensor Position Calibration and Direction Finding," *Proc. of IEEE National Radar Conference 1994*, pp. 155-159, 1994.

[34] S. Gazor, S. Affes, and Y. Grenier, "Wideband Multi-Source Beamforming with Adaptive Array Location Calibration and Direction Finding," *Proc. of IEEE ICASSP 1995*, vol. 3, pp. 1904-1907, 1995.

[35] Q.G.Liu, L.H.Zou, "Radio Direction Finding by Source Covariance Matrix Rotation," *Proc. of Intl. Symp. Antennas and Propagation Society*, vol. 1, pp. 270-273, 1988.

[36] P. Totarong and A.El-Jaroudi, "Robust High-Resolution Direction of Arrival Estimation via Signal Eigenvector Domain," *IEEE Journal of Oceanic Engineering*, vol. 18, no. 4, pp. 491-499, Oct. 1993.

[37] H.Lee, R. Stovall, "Maximum Likelihood Methods for Determining the Direction of Arrival for a Single Electromagnetic Source with Unknown Polarization," *IEEE Trans. Signal Processing*, vol. 42, no. 2, pp.474-479, Feb. 1994.

[38] M.Wax, J.Sheinvald, "Direction Finding of Choerent Signals via Spatial Smoothing for Uniform Circular Arrays," *IEEE Trans. Antennas and Propagation*, vol. 42, no. 5, pp. 613-620, May 1994.

[39] M.Wax, J.Sheinvald, A.J.Weiss, "Localization of Correlated and Uncorrelated Signals in Colored Noise via Generalized Least Squares," *Proc. IEEE ICASSP 1995*, vol. 3, pp. 2104-2107, 1995.

[40] M. Wax, J. Sheinvald, A.J. Weiss, "Detection and Localization in Colored Noise via Generalized Least Squares," *IEEE Trans. Signal Processing*, vol. 44, no. 7, pp. 1734-1743, July 1996.

[41] A.J.Weiss and B.Friedlander, "Direction Finding Via Joint Diagonalization," *Proc. of 8th IEEE Signal Processing Workshop on Statistical Signal and Array Processing*, pp. 66-69, 1996.

[42] T. Ratnarajah, "Mitigating the Effects of Array Uncertainties on the Performance of the Music Algorithm," *Proc. of 9th IEEE Signal Processing Workshop on Statistical Signal and Array Processing*, pp. 236-239, 1998.

[43] B.P. Flanagan, "Self Calibration of Antenna Arrays with Large Perturbation Errors," *PhD. Thesis*, George Mason University, Feb. 2000. Available at `http://www.galaxy.gmu.edu/~kbell/pubs/bflan.pdf`.

[44] A.J. Weiss and B. Friedlander, "Algorithm for Steering Vector Estimation Using Second Order Moments," *Proc. of 29th IEEE Asilomar Conf. On Sig., Syst., and Comp.*, pp. 782-786, Oct. 1995.

[45] P. Stoica and K. Sharman, "Maximum Likelihood Methods for Direction-of-Arrival Estimation," *IEEE Trans. Acoust., Speech, Signal Processing*, vol. 38, no. 7, pp. 1132-1143, July 1990.

[46] Ching-Yih Tseng, David D. Feldman, Lloyd J. Griffiths, "Steering Vector Estimation in Uncalibrated Arrays," *IEEE Trans. Signal Processing*, vol. 43, no. 6, pp. 1397-1412, June 1995.

[47] B.P. Flanagan and K.L. Bell, "Array Self Calibration with Large Sensor Position Errors," *Proc. of 33rd IEEE Asilomar Conf. On Sig., Syst., and Comp.*, pp. 258-261, Oct. 1999.

[48] B.P. Flanagan and K.L. Bell, "Improved Array Self Calibration with Large Sensor Position Errors For Closely Spaced Sources," *Proc. of 1st IEEE Sensor Array and Multichannel Signal Processing Workshop*, pp. 484-488, Mar. 2000.